

3. J. Hemberger *et al.*, *Nature* **434**, 364 (2005).
4. N. Hur *et al.*, *Nature* **429**, 392 (2004).
5. H. Gleiter, J. Weissmüller, O. Wollersheim, R. Würschum, *Acta Mater.* **49**, 737 (2001).
6. See, for example, the special issue on double layer modeling: *Electrochim. Acta* **41**, 2069 (1996).
7. J. Weissmüller *et al.*, *Science* **300**, 312 (2003).
8. Materials and methods are available as supporting material on *Science Online*.
9. G. H. O. Daalderop, P. J. Kelly, M. F. H. Schuurmans, *Phys. Rev. B* **44**, 12054 (1991).
10. Y. Chernyak, *J. Chem. Eng. Data* **51**, 416 (2006).
11. S. Okamoto *et al.*, *Phys. Rev. B* **67**, 094422 (2003).
12. We thank the Joseph Fourier University in Grenoble and the French Ministry of National Education for financial support. Part of this work was also supported by the Deutsche Forschungsgemeinschaft under grant FA 453/1.

## Supporting Online Material

www.sciencemag.org/cgi/content/full/315/5810/349/DC1

Materials and Methods

Figs. S1 to S3

References

23 October 2006; accepted 30 November 2006  
10.1126/science.1136629

# Ultralow Thermal Conductivity in Disordered, Layered WSe<sub>2</sub> Crystals

Catalin Chiritescu,<sup>1</sup> David G. Cahill,<sup>1\*</sup> Ngoc Nguyen,<sup>2</sup> David Johnson,<sup>2</sup> Arun Bodapati,<sup>3</sup> Pawel Koblinski,<sup>3</sup> Paul Zschack<sup>4</sup>

The cross-plane thermal conductivity of thin films of WSe<sub>2</sub> grown from alternating W and Se layers is as small as 0.05 watts per meter per degree kelvin at room temperature, 30 times smaller than the *c*-axis thermal conductivity of single-crystal WSe<sub>2</sub> and a factor of 6 smaller than the predicted minimum thermal conductivity for this material. We attribute the ultralow thermal conductivity of these disordered, layered crystals to the localization of lattice vibrations induced by the random stacking of two-dimensional crystalline WSe<sub>2</sub> sheets. Disordering of the layered structure by ion bombardment increases the thermal conductivity.

Materials with the lowest thermal conductivity are typically found among electrically insulating amorphous solids and glasses. In these materials, heat conduction is adequately predicted by a simple phenomenological model, the minimum thermal conductivity, in which heat conduction is described by a random walk of vibrational energy on the time and length scales of atomic vibrations and interatomic spacings (*l*). More sophisticated theories of heat conduction in disordered materials support this description: A majority of the vibrational modes [termed “diffusons” by Allen and Feldman (2)] carry heat in this manner, and only a small fraction of the vibrational modes propagate as waves or are localized and therefore unable to contribute to heat conduction. Recently, we (3) and others (4) have shown that the minimum thermal conductivity can be circumvented in multilayer thin films of metals and oxides. When the spacing between the interfaces is only a few nanometers, the thermal resistance of the interfaces reduces the thermal conductivity far below the thermal conductivity of the homogeneous amorphous oxide.

Here, we demonstrated by both experiment and computer simulation an alternative route for achieving ultralow thermal conductivity in a dense solid. The thermal conductivity of disordered thin films of the layered crystal WSe<sub>2</sub>

can be as small as 0.05 W m<sup>-1</sup> K<sup>-1</sup>, a factor of 6 smaller than the predicted minimum thermal conductivity and, to the best of our knowledge, the lowest thermal conductivity ever observed in a fully dense solid. Disruption of the layered structure and the crystallinity of the WSe<sub>2</sub> sheets by ion irradiation actually produces a marked increase in the thermal conductivity of the thin film. Thus, the lowest thermal conductivities are not found in the fully amorphous form of WSe<sub>2</sub>; rather, ultralow thermal conductivity is achieved by controlling both order and disorder, and hence the thermal pathways, in this anisotropic material.

We synthesized WSe<sub>2</sub> thin films by the modulated elemental reactants method (5, 6). Sequential bilayers of W and Se were deposited in an ultrahigh vacuum chamber onto unheated Si (100) wafers with a stoichiometry of 1:2 and then annealed for 1 hour at elevated temperatures in N<sub>2</sub> atmosphere to form the desired layered structures (6). The microstructure of the films was stable at room temperature. In the WSe<sub>2</sub> structure, a hexagonal plane of W atoms is bonded to two Se layers by strong covalent-ionic bonds, and each two-dimensional (2D) WSe<sub>2</sub> sheet is bonded to adjacent sheets by weaker van der Waals forces (7, 8). We purchased a single crystal of WSe<sub>2</sub> from Nanoscience Instruments to provide a baseline for comparisons. Thermal conductivity was measured by time-domain thermoreflectance (TDTR) (6, 9–12). In our implementation of TDTR, we determine the thermal conductivity by comparing the time dependence of the ratio of the in-phase  $V_{in}$  and out-of-phase  $V_{out}$  signals from the radio-frequency lock-in amplifier to calculations made with the use of a thermal model (11). The thermal model has several parameters, but the thermal conductiv-

ity of the WSe<sub>2</sub> sample is the only important unknown.

We used synchrotron x-ray diffraction to characterize the microstructure of a typical WSe<sub>2</sub> film (Fig. 1). Data for (0 0 L) reflections (6) showed that the layering of the 2D WSe<sub>2</sub> sheets was very precise; the surface normal to each sheet (hexagonal *c* axis) was well aligned with the surface normal of the substrate, and the spacing between the centers of WSe<sub>2</sub> sheets was highly uniform at 0.66 nm. These highly textured films had completely random crystalline orientation in the *a*-*b* plane. We examined the crystalline structure of the film by scanning the diffraction intensity through reciprocal space where the (1 0 3) reflection intersected the Ewald sphere. The relatively narrow line width (0.06 in reciprocal lattice units) in the direction parallel to the surface, [h 0 3], gave a lateral coherence length of 23 nm (Fig. 1C). Scans through the

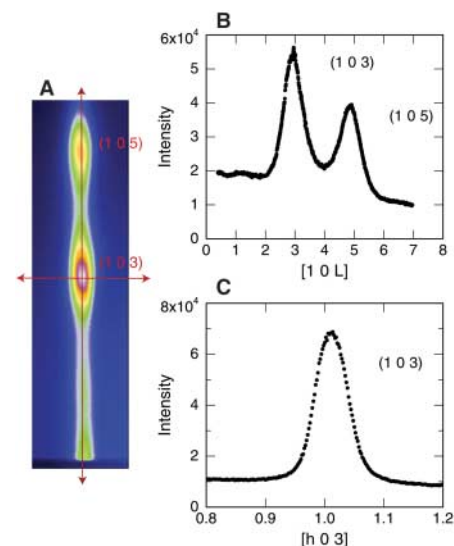


**Fig. 1.** X-ray diffraction data for a 32.5-nm-thick WSe<sub>2</sub> film collected at the 33-bending magnet beamline of the Advanced Photon Source with the use of 18.5-keV photons. After deposition, the WSe<sub>2</sub> film was annealed for 1 hour at 650°C in a N<sub>2</sub> atmosphere. (A) False-color depiction of the x-ray diffraction intensities collected by the area detector in the vicinity of the (1 0 3) and (1 0 5) reflections. The vertical direction is normal to the sample surface and the horizontal direction is in the plane of the sample. (B) Scan of the x-ray diffraction intensities along the surface normal. The scan direction is shown as the vertical red line in (A). (C) Scan of the x-ray diffraction in the in-plane direction. The scan direction is shown as the horizontal red line in (A).

<sup>1</sup>Department of Materials Science and Engineering, Frederick Seitz Materials Research Laboratory, University of Illinois, Urbana, IL 61801, USA. <sup>2</sup>Department of Chemistry, University of Oregon, Eugene, OR 97403, USA. <sup>3</sup>Department of Materials Science and Engineering, Rensselaer Polytechnic Institute, Troy, NY 12180, USA. <sup>4</sup>Advanced Photon Source, Argonne National Laboratory, Argonne, IL 60439, USA.

\*To whom correspondence should be addressed. E-mail: d-cahill@uiuc.edu

intersection of (1 0 L) reflections with the Ewald sphere probed the coherence of the crystal structure along the direction normal to the WSe<sub>2</sub> sheets. The large line widths (Fig. 1B) indicated that crystallographic ordering in the stacking of the WSe<sub>2</sub> sheets was limited to <2 nm.

We next compared the thermal conductivity of annealed WSe<sub>2</sub> films to the conductivity of a single crystal of WSe<sub>2</sub> and the predicted minimum thermal conductivity (Fig. 2). The thermal conductivity of single-crystal WSe<sub>2</sub> was approximately proportional to 1/T (the reciprocal of absolute temperature), as expected for a dielectric or semiconductor in which heat transport is dominated by phonons with mean-free paths limited by anharmonicity. Calculations of the minimum thermal conductivity require knowledge of the number density of atoms and the speed of sound (*I*). We used picosecond

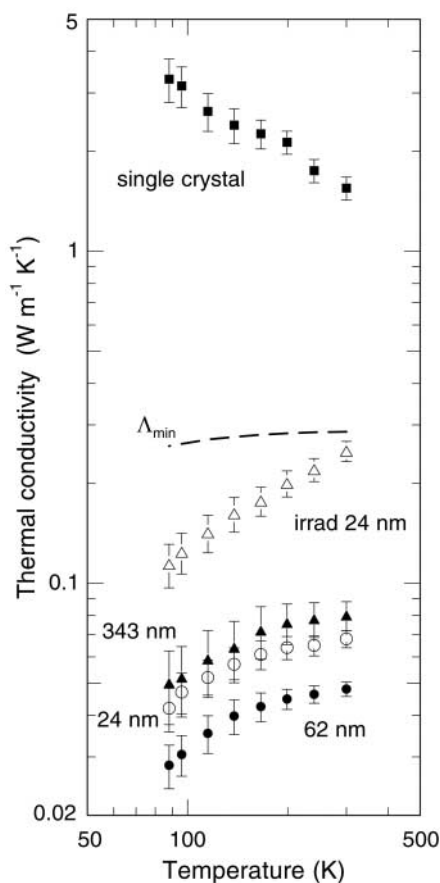


**Fig. 2.** Summary of measured thermal conductivities of WSe<sub>2</sub> films as a function of the measurement temperature. Each curve is labeled by the film thickness. Data for a bulk single crystal are included for comparison. Error bars are the uncertainties propagated from the various experimental parameters used to analyze the data (6). The ion-irradiated sample (irrad) was subjected to a 1-MeV Kr<sup>+</sup> ion dose of  $3 \times 10^{15} \text{ cm}^{-2}$ . The dashed line marked  $\Lambda_{\text{min}}$  is the calculated minimum thermal conductivity for WSe<sub>2</sub> films in the cross-plane direction.

acoustics to measure the longitudinal speed of sound in the cross-plane direction of nominal 360-nm-thick films and found that  $v_L = 1.6 \text{ nm ps}^{-1}$  (13, 14). This measurement is in good agreement with an independent measurement of the same film ( $v_L = 1.7 \text{ nm ps}^{-1}$ ) with the use of picosecond interferometry (15) and an index of refraction at the laser wavelength of 800 nm of  $n = 4.13$ . If we use the average of these values,  $v_L = 1.65 \text{ nm ps}^{-1}$ , and a mass density of  $\rho = 9.2 \text{ g cm}^{-3}$ , we obtain an elastic constant  $C_{33} = 25 \text{ GPa}$ , which is approximately a factor of 2 smaller than  $C_{33}$  for single crystals of NbSe<sub>2</sub> and TaSe<sub>2</sub> measured by neutron scattering (16) and single-crystal WSe<sub>2</sub> measured by picosecond interferometry. The transverse speed of sound  $v_T$  is not accessible to the standard methods of picosecond acoustics; instead, we estimated  $v_T = 1.15$  based on our measurement of  $v_L$  and the ratio  $C_{44}/C_{33}$  previously measured for NbSe<sub>2</sub> and TaSe<sub>2</sub> (16).

The lowest thermal conductivity,  $\Lambda$ , measured at 300 K is  $\Lambda = 0.048 \text{ W m}^{-1} \text{ K}^{-1}$  for a 62-nm-thick WSe<sub>2</sub> film, 30 times smaller than the cross-plane thermal conductivity of a single-crystal sample of WSe<sub>2</sub> (Fig. 2) and a factor of 6 smaller than the predicted minimum thermal conductivity. This degree of deviation from the predicted minimum thermal conductivity in a homogeneous material is unprecedented (17). Notably, the conductivity of the 62-nm-thick film is smaller than the conductivity of a thinner film (24 nm) or a thicker film (343 nm). The reasons for these differences are not understood in detail, but we speculate that variations in the degree of crystallographic ordering along the thickness of the films are playing an important role.

The data shown in Figs. 1 and 2 lead us to conclude that the ultralow thermal conductivities are produced by random stacking of well-crystallized WSe<sub>2</sub> sheets. To test this idea, we used irradiation by energetic heavy ions to dis-

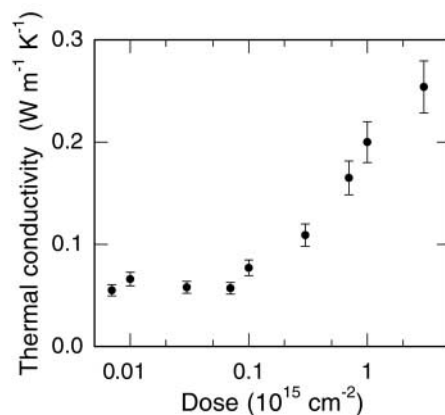


**Fig. 3.** Thermal conductivity versus irradiation dose for WSe<sub>2</sub> films 26 nm thick. Samples were irradiated with 1-MeV Kr<sup>+</sup> ions to the dose indicated on the *x* axis of the plot. Error bars are the uncertainties propagated from the various experimental parameters used to analyze the data (6).

rupt the crystalline order in the thin film samples (Fig. 3). Because our TDTR measurements require knowledge of the thermal conductivity of the substrate, bare silicon substrates were irradiated with the same range of ion fluences and measured by TDTR (6). At the highest ion dose,  $3 \times 10^{15} \text{ ions cm}^{-2}$ , we observed a factor of 5 increase in the thermal conductivity of the WSe<sub>2</sub> film. This increase in thermal conductivity with ion beam damage is also unprecedented. We inferred from these experiments that ion-induced damage introduces disorder that reduces localization of vibrational energy and enhances the transfer of vibrational energy in the material.

To gain further insight and confidence in our experimental results, we performed molecular dynamics (MD) simulations on model structures. For simplicity and computational efficiency, the atomic interactions in our model compound are described by 6-12 Lennard-Jones potentials:

$$U(r) = 4\epsilon \left[ \left( \frac{\sigma}{r} \right)^{12} - \left( \frac{\sigma}{r} \right)^6 \right] \quad (1)$$

where  $\epsilon$  is the energy scale and  $\sigma$  is the length scale. Two sets of  $\epsilon$  and  $\sigma$  parameters were used: For interactions within a single WSe<sub>2</sub> sheet,  $\epsilon = 0.91 \text{ eV}$  and  $\sigma = 2.31 \text{ \AA}$ , and for the interaction between layers,  $\epsilon = 0.08 \text{ eV}$  and  $\sigma = 3.4 \text{ \AA}$ . These parameters achieved a good fit to WSe<sub>2</sub> crystal structure and the  $C_{11}$  (200 GPa) and  $C_{33}$  (50 GPa) elastic constants. For computation efficiency, a cutoff of  $5.4 \text{ \AA}$  was used, with both energy and forces shifted such that they were zero at the

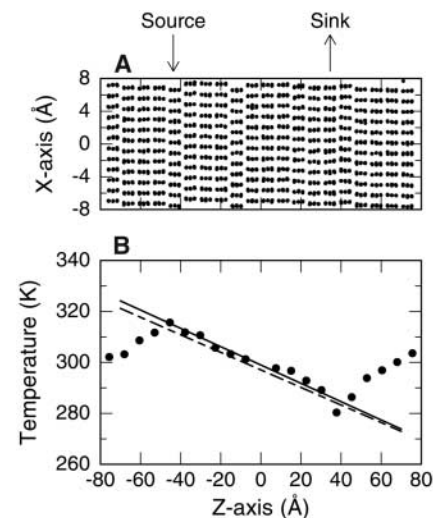


**Fig. 4.** (A) Atomic positions in a model WSe<sub>2</sub> structure showing stacking disorder. The positions of the heat sink and source separated by 8 nm are indicated. (B) The steady-state temperature profile obtained from the nonequilibrium, heat source-sink method. The solid line depicts a linear fit to the central region between the heat source and sink. The dashed line is an analogous fit but for the structure with doubled size along the *z* direction with the corresponding separation between the heat source and sink of 16 nm.

cutoff (18). The cross-sectional area of the simulation cell is  $15.3 \times 13.3 \text{ \AA}$ . Along the (001) direction, two sizes were selected: 160 and 320  $\text{\AA}$ . Periodic boundary conditions were used for all directions. Newton's equations of motions were solved by the fifth-order predictor corrector algorithm (18) with an MD time step,  $\Delta t = 1.8 \times 10^{-15} \text{ s}$ .

The simulation cell for the thermal transport measurement is depicted in Fig. 4. To calculate the thermal conductivity, we first equilibrated the structure at  $T = 300 \text{ K}$  for 100,000 MD time steps. Next, the global thermostat was turned off and thermal energy was added to one WSe<sub>2</sub> sheet and removed from a second sheet, which was located at a distance from the first sheet equal to one-half of the size of the simulation cell along the (001) direction (19, 20). Atomic velocities were scaled such that heat was added or subtracted at a constant rate,  $10^{-6} \text{ eV}$  per MD time step (21). We monitored the temperature profile by averaging the kinetic energy of atoms in each WSe<sub>2</sub> sheet. Because of the small energy barrier for shearing of the WSe<sub>2</sub> structure and the small cross-sectional area of the simulation cell, our model structures exhibited thermally excited local shearing events leading to disorder in the stacking of the WSe<sub>2</sub> sheets (Fig. 4).

After 5 to 20 million MD steps (depending on the system size), a steady-state temperature distribution was established (Fig. 4). The temperature gradient, and thus the thermal conductivity, of 16- and 32-nm-long simulation cells were essentially the same within the statistical standard

deviation of 10%,  $\Lambda = 0.06 \text{ W m}^{-1} \text{ K}^{-1}$ . Given the approximate form of the potentials used in our computational work, the agreement between the measured and calculated thermal conductivities was better than we expected. Nevertheless, the low thermal conductivity of the model structure suggests that the ultralow thermal conductivity in disordered, layered crystals is a general phenomenon and not restricted to WSe<sub>2</sub>.

Our WSe<sub>2</sub> films are poor electrical conductors in the cross-plane direction; however, if semiconductors with similar structural features and good electrical mobility can be identified, disordered layered crystals may offer a promising route to improved materials for thermoelectric energy conversion.

#### References and Notes

- D. G. Cahill, S. K. Watson, R. O. Pohl, *Phys. Rev. B* **46**, 6131 (1992).
- P. B. Allen, J. L. Feldman, *Phys. Rev. B* **48**, 12581 (1993).
- R. M. Costescu, D. G. Cahill, F. H. Fabreguette, Z. A. Sechrist, S. M. George, *Science* **303**, 989 (2004).
- Y. S. Ju, M.-T. Hung, M. J. Carey, M.-C. Cyrille, J. R. Childress, *Appl. Phys. Lett.* **86**, 203113 (2005).
- S. Moss, M. Noh, K. H. Jeong, D. H. Kim, D. C. Johnson, *Chem. Mater.* **8**, 1853 (1996).
- Materials and methods are available as supporting material on Science Online.
- W. J. Schutte, J. L. De Boer, F. Jellinek, *J. Solid State Chem.* **70**, 207 (1987).
- J. A. Wilson, A. D. Yoffe, *Adv. Phys.* **18**, 193 (1969).
- C. A. Paddock, G. L. Eesley, *J. Appl. Phys.* **60**, 285 (1986).
- R. J. Stoner, H. J. Maris, *Phys. Rev. B* **48**, 16373 (1993).

- D. G. Cahill, *Rev. Sci. Instrum.* **75**, 5119 (2004).
- D. G. Cahill, F. Watanabe, *Phys. Rev. B* **70**, 235322 (2004).
- K. E. O'Hara, X. Hu, D. G. Cahill, *J. Appl. Phys.* **90**, 4852 (2001).
- H. T. Grahn, H. J. Maris, J. Tauc, *IEEE J. Quantum Electron.* **25**, 2562 (1989).
- H.-N. Lin, R. J. Stoner, H. J. Maris, J. Tauc, *J. Appl. Phys.* **69**, 3816 (1991).
- D. E. Moncton, J. D. Axe, F. J. DiSalvo, *Phys. Rev. B* **16**, 801 (1977).
- P. A. Medwick, R. O. Pohl, *J. Solid State Chem.* **133**, 44 (1997).
- M. P. Allen, D. J. Tildesley, *Computer Simulation of Liquids* (Oxford Univ. Press, New York, 1987).
- A. Maiti, G. D. Mahan, S. T. Pantelides, *Solid State Commun.* **102**, 517 (1997).
- P. K. Schelling, S. R. Phillpot, P. Keblinski, *Phys. Rev. B* **65**, 144306 (2002).
- P. Jund, R. Jullien, *Phys. Rev. B* **59**, 13707 (1999).
- Supported by Office of Naval Research grant nos. N00014-05-1-0250 and N00014-96-0407. Research for this work was performed in the Laser and Spectroscopy Facility and the Center for Microanalysis of Materials of the Frederick Seitz Materials Research Laboratory, University of Illinois, which is partially supported by the U.S. Department of Energy under grant DEF02-91-ER45439. Use of the Advanced Photon Source was supported by the U.S. Department of Energy, Office of Science, Office of Basic Energy Sciences, under contract no. W-31-109-ENG-38.

#### Supporting Online Material

www.sciencemag.org/cgi/content/full/1136494/DC1  
Materials and Methods  
Figs. S1 to S5  
References

19 October 2006; accepted 4 December 2006  
Published online 14 December 2006;  
10.1126/science.1136494  
Include this information when citing this paper.

## Organic Glasses with Exceptional Thermodynamic and Kinetic Stability

Stephen F. Swallen,<sup>1</sup> Kenneth L. Kearns,<sup>1</sup> Marie K. Mapes,<sup>1</sup> Yong Seol Kim,<sup>1</sup> Robert J. McMahon,<sup>1</sup> M. D. Ediger,<sup>1\*</sup> Tian Wu,<sup>2</sup> Lian Yu,<sup>2</sup> Sushil Satija<sup>3</sup>

Vapor deposition has been used to create glassy materials with extraordinary thermodynamic and kinetic stability and high density. For glasses prepared from indomethacin or 1,3-bis-(1-naphthyl)-5-(2-naphthyl)benzene, stability is optimized when deposition occurs on substrates at a temperature of 50 K below the conventional glass transition temperature. We attribute the substantial improvement in thermodynamic and kinetic properties to enhanced mobility within a few nanometers of the glass surface during deposition. This technique provides an efficient means of producing glassy materials that are low on the energy landscape and could affect technologies such as amorphous pharmaceuticals.

Glassy materials combine the disordered structure of a liquid with the mechanical properties of a solid. Amorphous systems can be described in terms of a potential energy landscape, with thermodynamics and kinetics controlled by the minima and barriers on the landscape, respectively (1–3). Many im-

portant issues could be addressed if liquids or glasses with very low energies could be created (2, 4–6). For example, it might be possible to definitively understand the Kauzmann entropy crisis, an area of intense recent interest (1, 7–11). Kauzmann observed that if the entropy of many supercooled liquids is extrapolated to low temperature, the amorphous state is predicted to have a lower entropy than that of the highly ordered crystal well above absolute zero (5, 6).

Glasses are usually prepared by cooling a liquid, but accessing low energy states by this route is impractically slow (4, 12). If a liquid avoids crystallization as it is cooled, molecular

motion eventually becomes too slow to allow the molecules to find equilibrium configurations. This transition to a nonequilibrium state defines the glass transition temperature  $T_g$ . Glasses are “stuck” in local minima on the potential energy landscape (2, 3). Because glasses are thermodynamically unstable, lower energies in the landscape are eventually achieved through molecular rearrangements. However, this process is so slow that it is generally impossible to reach states deep in the landscape by this route.

We have discovered that vapor deposition can bypass these kinetic restrictions and produce glassy materials that have extraordinary energetic and kinetic stability and unusually high densities. We demonstrate this for two molecular glass formers: 1,3-bis-(1-naphthyl)-5-(2-naphthyl)benzene (TNB) ( $T_g = 347 \text{ K}$ ) and indomethacin (IMC) ( $T_g = 315 \text{ K}$ ). For these systems, the most stable glasses are obtained when vapor is deposited onto a substrate controlled near  $T_g - 50 \text{ K}$ . We argue that surface mobility during the deposition process is the mechanism of stable glass formation.

Differential scanning calorimetry (DSC) was used to examine the kinetics and thermodynamics of vapor-deposited samples created by heating crystalline TNB or IMC in a vacuum. Figure 1A shows DSC data for TNB vapor-deposited (blue) onto a substrate held at 296 K.

<sup>1</sup>Department of Chemistry, University of Wisconsin–Madison, Madison, WI 53706, USA. <sup>2</sup>School of Pharmacy, University of Wisconsin–Madison, Madison, WI 53705, USA. <sup>3</sup>Center for Neutron Research, National Institute of Standards and Technology, Gaithersburg, MD 20899, USA.

\*To whom correspondence should be addressed. E-mail: ediger@chem.wisc.edu